

# A Parallel CPU-GPU Framework for Cost-Bounded DFS with Applications to IDA\* and BTS

Ehsan Futuhi<sup>1</sup>, Nathan R. Sturtevant<sup>1,2</sup>

<sup>1</sup>University of Alberta, <sup>2</sup>Alberta Machine Intelligence Institute (Amii)  
{futuhi, nathanst}@ualberta.ca

## Abstract

The rapid advancement of GPU technology has unlocked powerful parallel processing capabilities, creating new opportunities to enhance classic search algorithms. A recent successful application of GPUs is in compressing large pattern database (PDB) heuristics using neural networks while preserving heuristic admissibility. However, very few algorithms have been designed to exploit GPUs during search. Several variants of A\* exist that batch GPU computations. In this paper we introduce a method for batching GPU computations in depth first search. In particular, we describe a new cost-bounded depth-first search (CB-DFS) method that leverages the combined parallelism of modern CPUs and GPUs. This is used to create algorithms like *Batch IDA\**, an extension of the Iterative Deepening A\* (IDA\*) algorithm, or Batch BTS, an extensions of Budgeted Tree Search. Our approach builds on the general approach used by Asynchronous Parallel IDA\* (AIDA\*), while maintaining optimality guarantees. We evaluate the approach on the 3x3 Rubik’s Cube and 4x4 sliding tile puzzle (STP), showing that GPU operations can be efficiently batched in DFS. Additionally, we conduct extensive experiments to analyze the effects of hyperparameters, neural network heuristic size, and hardware resources on performance.

## Introduction

In recent years, there has been exponential growth in computational resources, particularly in GPUs (Dally, Keckler, and Kirk 2021; Rotem et al. 2022). Modern CPUs also continue to evolve with enhanced parallel processing capabilities, enabling faster execution of complex algorithms. Simultaneously, GPUs have become indispensable for computation-intensive tasks due to their massive parallelism, capable of performing millions of operations simultaneously. This rapid advancement in both CPU and GPU technologies has been well exploited in many fields of Artificial Intelligence, especially deep learning (Schrittwieser et al. 2020; Yao et al. 2024).

How can classic search algorithms such as Iterative Deepening A\* (IDA\*) (Korf 1985) and more modern algorithms like Budgeted Tree Search (BTS) (Helmert et al. 2019; Sturtevant and Helmert 2020) benefit from this growth in technology? Several approaches (Li et al. 2022; Zhou and Zeng 2015; Agostinelli et al. 2019, 2024) have been developed to enhance search algorithms using the parallel pro-

cessing capabilities of modern GPUs. Li et al. (2022) introduced the first admissible neural network heuristic that compresses a large pattern database (PDB) heuristic with less information loss than standard compression techniques (Felner et al. 2007; Helmert, Sturtevant, and Felner 2017). *Batch A\** (Li et al. 2022) was then designed to use the admissible heuristic to find optimal solutions. Batch A\* is a variant of the A\* algorithm (Hart, Nilsson, and Raphael 1968), collecting states into batches to evaluate their heuristics through a single neural network lookup. This technique, called *batch heuristic evaluations*, utilizes GPU parallelism and significantly improves performance over performing individual neural network lookups for each state. However, Batch A\* remains slower than the plain A\* algorithm that uses PDB heuristics. Agostinelli et al. (2019) introduced the Batch Weighted A\* (BWA\*) algorithm, which combines weighted A\* search (Pohl 1970; Ebdend and Drechsler 2009) with batch heuristic evaluations.

Because algorithms like BTS and IDA\* are both designed around cost-bounded depth-first search (CB-DFS), the aim of this paper is to design a parallel CPU/GPU implementation of CB-DFS to efficiently use neural network heuristics during search. We demonstrate *CB-DFS* inside Batch IDA\* has two distinct phases working together: *search* and *heuristic evaluation*. The search phase is modified from the AIDA\* algorithm (Reinefeld and Schneck 1994), utilizing CPU parallelism to asynchronously generate and explore different subtrees in CB-DFS. Meanwhile, the heuristic evaluation phase continuously collects nodes generated by all subtrees into batches, which are then processed by the heuristic model on the GPU.

We then prove that using CB-DFS inside Batch IDA\* still guarantees the discovery of optimal solutions. In our experimental setting, IDA\* and BTS behave identically, so we only formulate and evaluate Batch IDA\*. We show that Batch IDA\* outperforms Batch A\* and performs comparably to AIDA\* in the Rubik’s Cube domain. In addition, we show that scaling the number of GPUs accelerates Batch IDA\* by enabling simultaneous evaluations.

## Related Work

In recent years, several parallel versions of the IDA\* algorithm have been introduced. AIDA\* (Reinefeld and Schneck 1994), a highly parallel iterative-deepening search al-

gorithm, was designed for large-scale asynchronous Multiple Instruction, Multiple Data (MIMD) systems. The algorithm partitions the search space and processes it asynchronously across multiple CPU processors. Taking a different approach, Horie and Fukunaga (2017) investigate the parallelization of IDA\* on GPUs using a block-based approach. The proposed Block-Parallel IDA\* (BPIDA\*) assigns subtrees to blocks of threads that execute on the same *streaming multiprocessors* (SMs). BPIDA\* takes advantage of local shared memory of within a SM to reduce warp divergence and improve load balancing.

GPU parallelism has also been effectively utilized in other search algorithms. Zhou and Zeng (2015) introduced the first parallel variant of the A\* search algorithm called GA\* that leverages the computational power of GPUs. GA\* uses multiple parallel priority queues to manage the Open list, enabling the simultaneous extraction and expansion of nodes across GPU threads. The heuristic computations are also parallelized across the GPU cores to optimize performance further. GA\* is up to 45x faster than a traditional CPU-based A\* implementations in large and complex search spaces. Q\* search (Agostinelli et al. 2024) employs deep Q-networks to calculate combined transition costs and heuristic values for child nodes in a single forward pass, thereby eliminating the need to explicitly generate them.

Edelkamp and Sulewski (2009) investigate bitvector-based search algorithms, where the GPU’s parallel processing capabilities allow for the efficient handling of state expansion and duplicate detection. The GPU is also employed for ranking and unranking permutations, computing hash functions, and managing the search frontier, all of which are parallelized to exploit the GPU’s architecture. Meanwhile, other approaches have formulated A\* and weighted A\* algorithms as differentiable and end-to-end trainable neural network planners (Yonetani et al. 2021; Archetti, Cannici, and Matteucci 2021). These data-driven approaches, rather than learning the heuristic function, take a raw image as an input and convert it to a guidance map by an encoder. GPUs have also been instrumental in learning heuristics. For example, Li et al. (2022) developed an admissible heuristic for the sliding tile puzzle (STP) and TopSpin using an ensemble of neural networks and classifier quantiles. Other approaches (Agostinelli et al. 2021; Arfaee, Zilles, and Holte 2011; Thayer, Dionne, and Ruml 2011; Pándy et al. 2022) have also focused on heuristic learning, though without guaranteeing admissibility.

## Background

In *heuristic search*, the task is to find a path in a graph  $\{G = \{V, E\}, s, g, c, h\}$  from a start state  $s \in V$  to a goal state  $g \in V$ , where  $c : E \rightarrow \mathbb{R}^+$  is a cost function associated with the edges between states. The heuristic function  $h(v)$  provides an estimate of the distance from a state  $v$  to the goal  $g$ . The heuristic is considered *admissible* if, for all states  $v$ ,  $h(v)$  does not exceed the true shortest distance  $h^*(v)$  to the goal. It is *consistent* if, for any two states  $a$  and  $b$ , the heuristic satisfies  $h(a) \leq c(a, b) + h(b)$ . In large state spaces, the graph  $G$  is represented implicitly, meaning it is generated online by expanding states and exploring their neighbors. A\*

and IDA\* are guaranteed to find optimal solutions when the heuristic is admissible.

## Heuristics

Pattern Database (PDB) heuristics are widely utilized in problems that exhibit exponential growth. These heuristics abstract the original graph  $V$  into a reduced state space  $\phi(V)$ . In this abstract space, edges between vertices in the original graph are preserved in the abstracted graph, meaning if an edge exists between  $v_1$  and  $v_2$  in  $V$ , a corresponding edge will exist between  $\phi(v_1)$  and  $\phi(v_2)$  in  $\phi(V)$ . As a result, abstract distances are admissible estimates of distances in  $V$ . PDBs can reduce the size of the state space exponentially with only a small loss in heuristic accuracy (Felner, Sturtevant, and Schaeffer 2009).

Standard PDB compression methods (Felner et al. 2007; Helmert, Sturtevant, and Felner 2017) primarily treat the PDB as a table of numbers. These methods group entries to reduce the PDB’s size and replace each entry in a group with the smallest value in that group to ensure the heuristic remains admissible. One common method is *DIV*, where  $k$  adjacent entries are grouped by dividing the index by  $k$ . Another method is *MOD*, which combines entries offset by  $\frac{m}{k}$  in a PDB with  $m$  total entries using the modulo operator.

Neural networks have been used to compress PDB heuristics. ADP (Samadi et al. 2008) utilizes a diverse range of techniques to uphold admissibility. This includes a unique loss function to penalize overestimation more than underestimation, utilizing a decision tree to partition states into smaller groups, and employing ANNs at the end nodes of the decision tree, which only undergo training on subsets of the state space. Any states with inadmissible heuristics are then stored in a hash table. The batch algorithms described in this paper are orthogonal to the use ADP for heuristics, but ADP would likely need to be redesigned to work efficiently on modern GPU architectures.

Li et al. (2022) propose treating the learning of heuristics as a classification problem rather than using regression. They use two other techniques to guarantee admissibility. The first is to adjust the quantile of the distribution to select heuristic values by leveraging the ordered nature of classes. For instance, a quantile of 0.5 returns the first class that has a cumulative probability of 0.5 from small to large classes. By selecting a lower quantile, the network can generate conservative estimates that are less likely to overestimate the cost to the goal. The second is to use an ensemble of neural networks. Each network in the ensemble generates its own heuristic estimate, and the minimum of these estimates is used as the final heuristic value. This technique leverages the diversity of the ensemble to produce an admissible heuristic.

## A\*, IDA\* and BTS

IDA\* combines a cost-bounded depth-first search (CB-DFS) with iterative deepening to find optimal solutions. IDA\* performs a series of depth-first searches, each with an increasing cost threshold, which is determined by the current path cost and the heuristic estimate to the goal. The algorithm starts with an initial threshold set to the heuristic estimate of the start node. It explores all paths in a depth-first order with

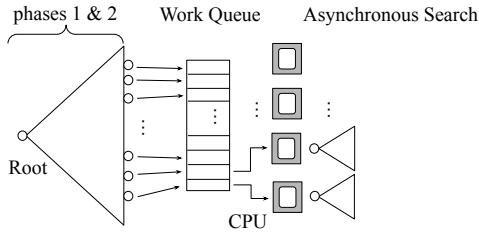


Figure 1: The structure of AIDA\*.

costs less than or equal to this threshold. If the goal is not found, the threshold is increased to the minimum cost that exceeds the current threshold. This process is repeated until the goal is reached. IDA\* is memory-efficient, as it only requires storage for the current path. However, if the number of nodes in each iteration does not grow fast enough, the cost of the iterations may outweigh the cost of the final iteration, increasing the total expansions from  $O(N)$  to  $O(N^2)$ . BTS Helmert et al. (2019) is a variant of IBEX which is identical to IDA\* when the iterations grow by a suitable constant factor, but reduces the worst-case overhead to  $O(N \log C^*)$ , where  $C^*$  is the optimal solution cost. As in IDA\*, BTS repeatedly invokes CB-DFS, just with more aggressive thresholds and node expansion limits. Thus, both IDA\* and BTS can be improved through GPU parallelization of CB-DFS.

## AIDA\*

AIDA\* parallelizes the CB-DFS portion of IDA\* in three key phases (as shown in Figure 1):

- **Initial Data Partitioning:** In this phase, all processors work in parallel to redundantly expand the initial few levels of the search tree using an iterative-deepening approach. This generates sufficient nodes to ensure that each processor has enough work for the next phase. At the end of this phase, duplicate nodes are eliminated from the frontier nodes.
- **Distributed Node Expansion:** Each processor is assigned a set of nodes from the first phase, expanding these nodes further to create a larger set. At the end of this phase, the local node arrays of the individual processors make up the global work queue used for dynamic load balancing in the third phase. Each work packet in the work queue is the root of a subtree to be explored in the next phase.
- **Asynchronous Search:** In this phase, processors independently and asynchronously explore different subtrees of the search space using an iterative-deepening strategy. Each processor continues working on its assigned subtree until either a solution is found or the subtree is fully explored. Since the work queue is shared among all threads, idle threads dynamically retrieve unprocessed work packets from the queue as they complete their current assignments, ensuring continuous utilization of all processing resources.

## GPU Architecture

GPUs use a hierarchical execution model that enhances parallel processing efficiency. At the heart of this model is the *kernel*, which executes across multiple thread blocks. Each block contains warps, groups of threads that execute the same instructions in parallel. Threads within a block can share data through on-chip memory, but blocks themselves work independently without direct communication.

The architecture of GPUs is designed to support this model, with each GPU featuring multiple *Streaming Multiprocessors* (SMs). These SMs include on-chip memory, *shader cores*, and *warp schedulers*. Shader cores handle arithmetic and logic operations, while warp schedulers manage the execution of warps, selecting which ones are ready to execute in each cycle. GPUs can be connected to systems either via the PCI-E bus, as in Ubuntu servers, or integrated on the same processor package as the CPU, like in Apple’s M1 or M2 chips. When connected through PCI-E, GPUs typically have dedicated memory, necessitating explicit data transfers between CPU and GPU memory.

CPUs excel at tasks with complex control flows and high instruction-level parallelism, making them ideal for sequential tasks. In contrast, GPUs are optimized for handling large, independent data sets, which makes them especially effective for neural network computations. In convolutional neural networks (CNNs), for example, a weight matrix and a subset of inputs are assigned to a thread block, where threads compute convolution outputs by sharing data through fast on-chip memory. Since different convolution operations are independent of each other, they can be executed in parallel *batches* across multiple thread blocks (Jeon 2023). This data-level parallelism gives GPUs a significant advantage over CPUs in neural network training and inference.

## Batch A\*

Batch A\* (Li et al. 2022) is a modification of A\* that allows it to delay node heuristic evaluation when using neural network heuristics. When nodes are generated, they are placed into a batch queue instead of the open list. Once the batch queue is full, the heuristics of the states in the batch are evaluated in parallel, and then they are inserted into the A\* open list for search to continue.

## Problem Definition

In a heuristic search problem, the heuristic,  $h$ , can come from any source. In this paper we are interested in the *neural heuristic search* problem. In this problem,  $h$  is a neural heuristic. This means that  $h \in H_{NN}$ , where  $H_{NN}$  is the set of all heuristics that are computed by a neural network. In recent work, heuristics in  $H_{NN}$  have been learned from PDB heuristics (Li et al. 2022), but we do not distinguish the source of the heuristic or how it was trained. Experimental results evaluate the quality of heuristics we currently have access to, but we are working under the assumption that neural network heuristics will continue to improve, and thus we should build and evaluate algorithms that can be efficiently used with such heuristics during search.

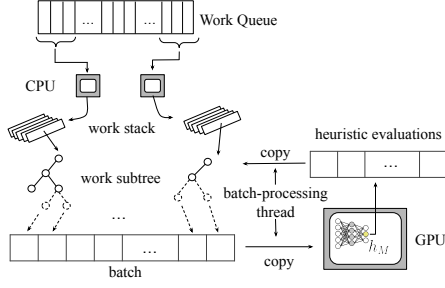


Figure 2: The structure of SingleGPU CB-DFS.

---

#### Algorithm 1: Batch IDA\*

---

```

1: Input:  $h_M$ , start  $s$ , goal  $g$ ,  $d_{init}$ 
2: works, history, batch  $\leftarrow \{\}$ 
3: bound  $\leftarrow h_M(s, g)$ 
4: foundSolution  $\leftarrow$  false
5: GenerateWork( $s, d_{init}$ , history)
6: start a batch-processing CPU thread executing ProcessBatch()
7: while not foundSolution do
8:   start search CPU threads executing CB-DFS(bound)
9:   wait for CB-DFS threads to end
10:  UpdateThreshold(bound)
11: end while

```

---

## Method

We now introduce the SingleGPU Batch IDA\* algorithm, provide its pseudocode, and prove its theoretical guarantees. Then, we discuss the MultiGPU Batch IDA\* algorithm. These algorithms are based on a CPU/GPU implementation of CB-DFS. Batch BTS has a different outer loop, but can use CB-DFS with an additional expansion limit. Since Batch IDA\* and Batch BTS perform identically in our setting, we present the ideas using the simpler Batch IDA\* setting. But, our approach parallelizes the common CB-DFS used by both, not the top-level control of IDA\* or BTS.

### SingleGPU Batch IDA\*

*SingleGPU Batch IDA\** extends AIDA\* by leveraging batch heuristic evaluations using a learned heuristic  $h_M$ . The algorithm builds the CB-DFS tree in a manner consistent with AIDA\*. It begins by replicating the first two phases of AIDA\* to generate a *Work Queue* for parallel processing. Each piece of work in the Work Queue represents a subtree rooted at a node generated during the initial phase. The remaining procedure of the algorithm is generally depicted in Figure 2. In each CB-DFS call, every thread retrieves several pieces of work from the Work Queue and stores them in a stack. Threads process each piece of work in depth-first order, generating new nodes as they traverse its subtree. Once a piece of work is completed—meaning all nodes in its subtree have been generated—the thread takes on a new one. CB-DFS completes when all threads have processed the work in their stacks under the current cost threshold and the Work Queue is empty.

The newly generated nodes from all threads are collected in a vector called *batch*. When the batch reaches its max-

---

#### Algorithm 2: Generate works for parallel CB-DFS

---

```

1: function GenerateWork( $s, d_{init}$ , history)
2:   if size(history) =  $d_{init}$  then
3:     work  $\leftarrow$  Work( $s$ )
4:     work.init  $\leftarrow$  history
5:     works.add(work)
6:   return
7: end if
8: actions  $\leftarrow$  env.GetActions( $s$ )
9: for each action in actions do
10:  history.add(action)
11:   $s \leftarrow$  env.ApplyAction( $s$ , action)
12:  GenerateWork( $s, d_{init}$ , history)
13:   $s \leftarrow$  env.UndoAction( $s$ , action)
14:  history.pop()
15: end for
16: end function

```

---



---

#### Algorithm 3: Parallel CB-DFS

---

```

1: function CB-DFS(bound)
2:   Initiate stack[workNum]
3:   Initialize terminated  $\leftarrow [0, 0, \dots, 0]$  of length workNum
4:   counter  $\leftarrow 0$ 
5:   miss  $\leftarrow 0$ 
6:   for  $i = 1$  to workNum do
7:     stack[i]  $\leftarrow$  works.pop()
8:   end for
9:   while miss < workNum do  $\triangleright$  wait for all works to be done
10:    if stack[counter] is done then
11:      if works is not empty then
12:        stack[counter]  $\leftarrow$  works.pop()
13:      else
14:        miss  $\leftarrow$  miss + 1
15:        terminated[counter]  $\leftarrow 1$ 
16:      end if
17:    end if
18:    if not terminated[counter] then
19:      DoIteration(stack[counter], bound)
20:    end if
21:    counter  $\leftarrow$  counter + 1
22:  end while
23: end function

```

---

imum size, a *batch-processing thread* manages it in three steps: copying the batch from the CPU to the GPU, performing heuristic lookup using the model  $h_M$ , and copying the heuristic evaluations back to the CPU. After assigning the evaluations to their nodes, the batch is cleared, allowing the next set of generated nodes to be processed.

The detailed steps of SingleGPU Batch IDA\* are outlined in Algorithm 1. The first two phases are executed via the **GenerateWork** function (line 5). This function is presented in Algorithm 2, which constructs the CB-DFS tree up to a depth of  $d_{init}$ . The third phase is managed by invoking the **CB-DFS** function in parallel across available CPU threads at each cost threshold (line 8). The cost threshold is updated (**UpdateThreshold** function) after the CB-DFS with the current threshold is completed (line 10).

The **CB-DFS** function (provided in Algorithm 3) has one primary change compared to **CB-DFS** function in AIDA\*.

---

**Algorithm 4: Subtree expansion**

---

```

1: function DoIteration(work, bound)
2:   newStatesFound  $\leftarrow$  false
3:   while not newStatesFound do
4:      $s \leftarrow$  work.GetTop()
5:     if  $h_M(s)$  is not ready then
6:       return
7:     end if
8:     if  $h_M(s, \text{goal}) < \text{bound}$  then
9:       newStatesFound  $\leftarrow$  true
10:    end if
11:  end while
12:  actions  $\leftarrow$  env.GetActions( $s$ )
13:  for each action in actions do
14:     $s_{next} \leftarrow$  env.ApplyAction( $s$ , action)
15:    work.add( $s_{next}$ )
16:    batch.add(TensorRepresentation( $s_{next}$ ))
17:  end for
18: end function

```

---

In AIDA\*, each thread processes one piece of work at a time and does not begin another until the current one is fully completed. However, applying this method to Batch IDA\* limits the maximum batch size:

$$\text{batch size} \leq \max_{s \in S} b(s) * n, \quad (1)$$

where  $b(s)$  is the branching factor of state  $s$  and  $n$  is the number of CPU threads. This limitation occurs because heuristic evaluations for successors aren't immediately ready, forcing the CB-DFS to wait for the completion of batch evaluation. This is restrictive, as large batch sizes are needed to fully utilize GPU parallelism. To overcome this, each thread needs to process multiple pieces of work altogether (Algorithm 3). For this purpose, each thread maintains a work stack, with the number of pieces specified by `workNum` (lines 6-8). This approach allows for larger batches by adjusting `workNum` while maintaining the same number of threads.

The `DoIteration` function (Algorithm 4) expands subtrees one at a time. While executing the `DoIteration` function, if a subtree cannot progress further—meaning the heuristic evaluation is not yet available for the top node (line 5)—the thread switches to the next subtree in its stack. Upon revisiting the same subtree, the thread resumes from the same node if its heuristic evaluation is ready; otherwise, it switches again to the next subtree.

The batch processing is done via the `ProcessBatch` function, as shown in Algorithm 5. In this function, we consider a `timeout` which invokes batch processing even if the batch is not full. This mechanism helps when only a few pieces of work remain and the number of generated nodes is insufficient to fill the batch.

Overall, the performance of Batch IDA\* hinges on the balance between two key events: *filling the batch* and *processing the batch*. The time required to fill the batch depends on the speed of the CPU CB-DFS threads, while processing time is determined by the GPU's efficiency and the transfer time via the PCI-E bus. If batch-filling is faster, CB-DFS

---

**Algorithm 5: Process of heuristic batch**

---

```

1: function ProcessBatch()
2:   wait for the batch to get full or for the timeout to expire
3:   copy batch from CPU to GPU
4:   results  $\leftarrow$   $h_M(\text{batch})$ 
5:   copy results from GPU to CPU
6:   return results
7: end function

```

---

threads may remain idle, either waiting to add new nodes or for heuristic evaluations. Conversely, if batch processing is faster, the GPU is underutilized. Therefore, these two processes must be balanced to ensure optimal resource utilization during the CB-DFS.

## Theory

In this section, we demonstrate that Batch IDA\* is guaranteed to find an optimal solution, assuming one exists. Our proof builds on the established optimality of IDA\*. Since the original AIDA\* paper lacks a formal proof of optimality, we begin by showing this guarantee for AIDA\* and then use this result to prove the optimality of Batch IDA\*.

**Lemma 1.** *Given an admissible monotone cost function, iterative-deepening- A\* will find a solution of least cost if one exists (Korf 1985).*

**Lemma 2.** *Let  $f$  be an admissible and monotone cost function. Then, the AIDA\* algorithm is guaranteed to find an optimal solution, provided that a solution exists.*

*Proof.* From Lemma 1, we know that IDA\* using the cost function  $f$  finds an optimal solution if a solution exists. Therefore, our task is to demonstrate that AIDA\*, using the same cost function  $f$  as IDA\*, expands all the nodes that IDA\* expands at each cost threshold. We know that, like IDA\*, AIDA\* does not increase the cost threshold until all nodes with costs below the current threshold have been expanded. Assume, for the sake of contradiction, that there exists a node  $s_{missed}$  that IDA\* expands but AIDA\* does not. Let us also assume that the initial phase in AIDA\* proceeds up to a depth of  $d_{init}$ . We select a path from the root to  $s_{missed}$ , denoted as  $path$ . The node  $s_{missed}$  falls into one of two categories:

1. The length of  $path$  is less than or equal to  $d_{init}$ .
2. The length of  $path$  exceeds  $d_{init}$ .

If  $s_{missed}$  falls within the first category, it must be expanded during initial phase, as this phase generates the entire tree up to  $d_{init}$  levels. Therefore, in this case,  $s_{missed}$  cannot be missed by AIDA\*. If  $s_{missed}$  falls into the second category, we can express the  $path$  as  $\{root, s_1, \dots, s_{d_{init}}, \dots, s_{missed}\}$ . The  $path$  intersects the tree generated in the initial phase at node  $s_{d_{init}}$ . We know that, during second and third phases, AIDA\* grows the subtree for all leaf nodes of the initial tree, including  $s_{d_{init}}$ . Since both AIDA\* and IDA\* use the same cost function  $f$ , the same cost threshold, and both employ a depth-first search strategy, AIDA\* is guaranteed to expand the node  $s_{missed}$ .

during subtree expansion of  $s_{d_{init}}$ . Thus, AIDA\* does not miss any node that IDA\* expands. This concludes the proof that AIDA\* will find an optimal solution if one exists.  $\square$

**Theorem 1.** *Let  $h_M$  be an admissible heuristic learned from a PDB heuristic  $h$ . Then, Batch IDA\* using  $h_M$  is guaranteed to find an optimal solution, assuming that a solution exists.*

*Proof.* From Lemma 2, we know that AIDA\*, using a PDB heuristic  $h$ , is guaranteed to find the optimal solution if a solution exists. To extend this guarantee to Batch IDA\*, we must demonstrate that CB-DFS, when using the learned heuristic  $h_M$  derived from  $h$ , does not omit any node expansions at any cost threshold. The primary difference between Batch IDA\* and AIDA\* lies in the heuristic computation. Therefore, we need to verify two properties:

1. *Heuristic Evaluation Completeness:* No node is expanded or discarded without having its heuristic properly evaluated. In CB-DFS, each thread switches to another subtree if the heuristic evaluation of the top node in its work is not yet available. The thread does not advance the subtree until the batch evaluation is complete and the heuristics are ready. This mechanism guarantees that every node is assessed using a valid heuristic  $h_M$ .
2. *Expansion Condition Alignment:* Given that  $h_M$  is an admissible heuristic, it inherently serves as a lower bound for the original PDB heuristic  $h$ :

$$h_M(s) \leq h(s) \quad \forall s \in S.$$

This inequality implies that if a node satisfies the expansion condition under AIDA\*, meaning  $h(s) + g(s) \leq \text{threshold}$ , it will also satisfy the expansion condition under the CB-DFS:  $h_M(s) + g(s) \leq \text{threshold}$ . Therefore, any node that qualifies for expansion in AIDA\* will also qualify in Batch IDA\*'s CB-DFS.

Since both properties hold, Batch IDA\* is guaranteed to find an optimal solution, assuming one exists.  $\square$

A similar argument extends to BTS, and any algorithm that uses our CPU/GPU-based CB-DFS.

## Memory Cost Analysis

The memory cost of IDA\* is  $\mathcal{O}(d)$ , where  $d$  is the solution depth (Korf 1985). For AIDA\*, which utilizes  $n$  CB-DFS threads, the memory cost increases to  $\mathcal{O}(dn)$  as it concurrently expands  $n$  subtrees. In Batch IDA\*'s CB-DFS, each thread manages  $k$  subtrees in a stack, resulting in a memory cost of  $\mathcal{O}(dnk)$ . We know that  $n$  and  $k$  are related to hardware speed on any domain. So, these parameters are expected to be constant as hardware is constant. Additionally, while the heuristic evaluations for unexpanded nodes are stored temporarily, memory is freed after their expansion, keeping the total memory cost at  $\mathcal{O}(dnk)$ .

Both AIDA\* and Batch IDA\* require loading their respective heuristics into memory. If AIDA\* uses a PDB heuristic  $h$  and Batch IDA\* uses a learned model  $h_M$ , the total memory cost for AIDA\* is  $\mathcal{O}(nd + \text{size}(h))$  and for

Batch IDA\*, it is  $\mathcal{O}(dnk + \text{size}(h_M))$ . While PDB heuristics typically fit into memory and thus their cost is constant and negligible, large PDBs, such as the 12-edge Rubik's cube PDB (500 GB), exceed memory capacity, making them impractical for AIDA\*. This limitation underscores the importance of compressing PDB heuristics using deep learning models (Li et al. 2022) and designing search algorithms, such as the CB-DFS used by Batch IDA\* and Batch BTS, to use them efficiently.

## MultiGPU Batch IDA\*

In most servers, multiple GPU devices are available; however, SingleGPU Batch IDA\* is limited to using one GPU device. This means that even if faster CPUs are employed for the search, overall performance gains are minimal because the batch processing time remains unchanged, forcing CB-DFS threads to wait until the model  $h_M$  is ready to take a new batch. A potential solution involves loading copies of  $h_M$  onto GPU, allowing multiple batches to be processed simultaneously. However, this can lead to oversubscription, where the GPU lacks sufficient SMs to efficiently handle all batches, potentially increasing runtime. To address this issue, we introduce *MultiGPU Batch IDA\** which leverages multiple GPU devices. In this approach,  $h_M$  is loaded onto each GPU, with a batch and a batch-processing thread assigned to each device. CB-DFS threads are distributed evenly across the GPUs, with each GPU processing the batch of nodes generated by its respective CB-DFS threads. This setup maximizes CPU utilization by increasing the number of batches while ensuring sufficient GPU resources are available to process them concurrently.

## Experimental Results

We evaluate the Batch IDA\* algorithm to understand its performance and how it compares to existing algorithms. Our first two experiments evaluate whether our Batch IDA\* design is effective in reducing the computational overhead of neural heuristics, and how the size of the neural heuristic model impacts performance. This is followed by an analysis of the impact of different hyperparameters and hardware. Finally, we perform a comparison between classical and neural heuristics to evaluate their current performance differences.

### Experimental Setup

We conduct our experiments across two domains: the 3x3 Rubik's cube and the 4x4 sliding tile puzzle (STP). We use relatively modest computational resources in our experiments. Specifically, we utilize a server equipped with 32 AMD Ryzen Threadripper 2950X CPU cores and two NVIDIA GeForce RTX 2080 Ti GPUs running CUDA version 12.4. The Batch IDA\* algorithm is implemented in C++, and Libtorch is employed for the deep learning components. Any CPU parallelization uses one thread per CPU core. For the non-learning algorithms, IDA\* and AIDA\*, we use  $h_{\text{PDB}}$  which is the 8-corners PDB for Rubik's cube, and the sum of 1-7 and 8-15 tile additive PDBs for STP. For the STP, we use standard benchmark instances (Korf 1985). For

Average Performance Over 50 Instances							
Algorithm	Batch Size	3x3 Rubik's Cube			4x4 STP		
		Time (s)	Expanded	Generated	Time (s)	Expanded	Generated
SingleGPU Batch IDA*	1	> 100	-	-	16.80	104,869	225,542
SingleGPU Batch IDA*	8	> 100	-	-	3.97	93,610	201,217
SingleGPU Batch IDA*	80	58.07	902,026	11,966,615	0.94	93,575	201,145
SingleGPU Batch IDA*	800	5.46	908,522	12,054,452	0.54	104,945	225,704
SingleGPU Batch IDA*	8,000	3.46	900,725	13,734,532	0.71	115,190	248,108
2GPU Batch IDA*	800	2.78	982,864	13,044,563	0.44	104,833	225,468
2GPU Batch IDA*	8,000	2.51	936,426	13,172,161	0.64	115,876	249,264
Batch A*	1,000	23.58	779,495	14,030,893	0.18	17,892	41,465

Table 1: Summary results comparing learning algorithms using the same PDB heuristic.

Average Time (s) Over 50 Instances				
Model size (MB)	SingleGPU Batch IDA*		Batch A*	
	RC	STP	RC	STP
0.2	3.46	0.52	11.16	0.18
2.3	4.75	0.78	16.71	0.29
13.6	10.23	1.45	20.66	0.38

Table 2: Impact of model size on Batch IDA\* speed.

Rubik’s cube, we generate instances by performing a random walk of length 11 to 13 starting from the goal. All PDB heuristics and baseline implementations are sourced from HOG2<sup>1</sup>. The heuristic  $h_M$  for the STP is the model introduced by Li et al. (2022). It is constructed by combining two ensemble models: the first is trained on the difference between the 1-7 tile PDB and the Manhattan distance heuristic, while the second is similarly trained using the 8-15 tile PDB. We also trained an admissible heuristic  $h_M$  using the 8-corners PDB for the Rubik’s Cube; however, a full description is outside the scope of this paper. But, what is important is that both approaches learn classifiers instead of using regression. Because of this, the IDA\* search layers are well-behaved. Learning with regression would result in a broader range of non-integer heuristic values, and thus require using BTS instead of IDA\*.

## Performance Evaluation

Our first experiment is designed to evaluate the effectiveness of batch operations in Batch IDA\*. We designed this experiment to isolate as many variables as possible in the experiment and to isolate the quality of neural heuristic from the mechanics of Batch IDA\*. We isolate the impact of neural heuristic training by using randomly initialized neural heuristics. This allows us to quickly experiment with different network topologies and sizes without having to re-train neural heuristics for every setting. While it is possible to use Batch IDA\* with random heuristics, this would introduce variance in tree sizes across heuristics. Additionally, random heuristics are highly inconsistent (Felner et al. 2011), which

introduces the potential for the worst-case time complexities for IDA\* and A\* (Helmert et al. 2019; Kaur and Sturtevant 2022). We avoid this by calculating the neural heuristic as if we were going to use it, but then replace the heuristic values with values from  $h_{PDB}$  to guide the CB-DFS.

Results of this experiment are presented in Table 1. Each algorithm is given 5000s to solve all problems in the problem set, or an average of 100s per problem. Batch IDA\* with a batch size of 1 or 8 fails to solve all of the Rubik’s Cube instances within the time limit. But, increasing the batch size to 8000 reduces the average time to 3.46s. Using two GPUs and a batch size of 8000 further reduces this to 2.51s, which is almost ten times faster than Batch A\*. Note that Batch A\* is only parallel on the GPU, not the CPU. Adding CPU parallelization to Batch A\* is an open challenge.

We use the first 50 instances from Korf’s benchmarks for the STP domain. On this domain, going from batch size of 1 to 800 reduces the running time from 16.80s to 0.54s, a 30× improvement. Using two GPUs and batch size 800 reduces this further to 0.44s. The variance in nodes expanded is due to a deep initial phase in Batch IDA\* aimed at producing sufficient work pieces, which results in batches containing extra nodes that are not necessary to solve the problem ( $f$ -cost greater than the threshold). Although Batch IDA\* is faster than Batch A\* with respect to time per node expansion, Batch A\* expands fewer nodes because it detects duplicates, which Batch IDA\* does not.

## Model Size

Our second experiment looks at the impact of model size on CB-DFS performance. We run Batch IDA\* on the same domains with a single GPU and the best parameters from Table 1. We vary the model size by fixing the number of layers, but changing the number of fully connected neurons in each layer. The results of this experiment are found in Table 2. These results show that increasing the size of the model does not linearly increase the time required to evaluate the model, although larger models are more expensive to evaluate. Thus, there will be trade-offs between model quality and speed when deploying neural heuristics.

The results also show that Batch A\* is less affected by model size than Batch IDA\*. The main reason for this difference is that the batches in Batch IDA\* are not always full,

<sup>1</sup><https://github.com/nathansttt/hog2/tree/PDB-refactor>



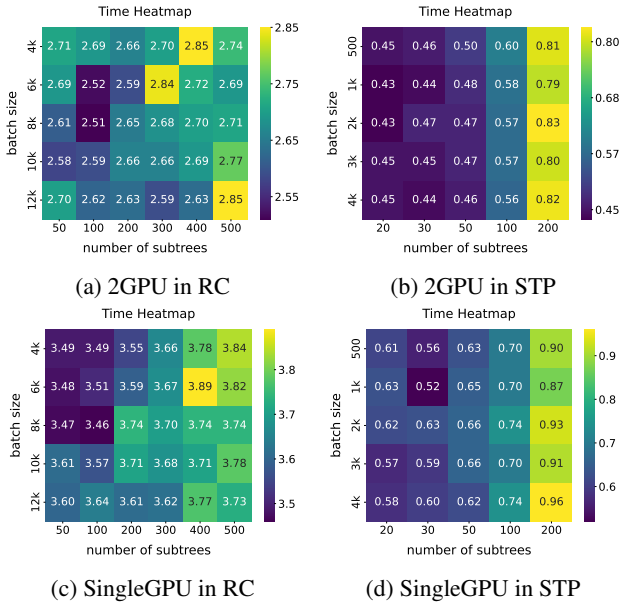


Figure 3: Hyperparameter analysis for Batch IDA\*.

Average Performance Over 50 Instances				
Algorithm	RC		STP	
	Time (s)	Generated	Time (s)	Generated
4GPU Batch IDA*	2.56	12,027,388	0.57	238,440
2GPU Batch IDA*	2.97	11,322,876	0.58	239,492
SingleGPU Batch IDA*	6.11	12,498,111	0.99	231,958
AIDA*	2.26	14,793,061	0.02	101,020

Table 3: Impact of GPU counts on Batch IDA\* performance.

meaning the GPU isn't being used as efficiently in Batch IDA\*. This can be caused by node generations above the cost thresholds and the uneven distribution of work between subtrees. When the model requires more time to evaluate, these issues are accentuated. See the Supplementary Material for more analysis of how full the batches are in practice.

## Hyperparameter Analysis

Next, we present the impact of hyperparameters on the performance of Batch IDA\*. For this experiment, we consider the batch size and the number of subtrees per thread, specified by `workNum` in Algorithm 3. The timing results for different combinations of hyperparameter values are shown in Figure 3. In Rubik's Cube there is only about 10% variation between the best and worst parameters, whereas in STP there is a  $1.84\times$  difference. The STP domain has less balanced subtrees than Rubik's Cube. With too many subtrees, the work is divided out to all threads too quickly, reducing the ability to load-balance between smaller and larger subtrees. The range of batch sizes did not have a large impact on performance. This is due to the timeout mechanism in place; if batch filling exceeds the timeout, the process is stopped, and the batch is processed with its current size.

Average Performance Over 50 Instances				
Algorithm	4*4 STP			
	batch size	Time (s)	Expanded	Generated
SingleGPU Batch IDA*	8000	13.11	777,652	1,598,045
2GPU Batch IDA*	8000	11.78	770,341	1,428,177
AIDA*	-	1.21	10,513,092	30,254,284
IDA*	-	4.23	8,180,928	17,639,025
Batch A*	1000	2.26	88,977	273,505

Table 4: STP results using a learned admissible heuristic.

Average Performance Over 50 Instances				
Algorithm	3*3 Rubik's cube			
	batch size	Time (s)	Expanded	Generated
2GPU Batch IDA*	8000	5.11	1,001,733	13,028,957
SingleGPU Batch IDA*	8000	8.06	1,005,874	13,082,769
AIDA*	-	2.74	2,218,215	29,401,255
IDA*	-	5.84	2,106,615	27,900,766
Batch A*	1000	42.07	779,491	14,030,761

Table 5: RC results using a learned admissible heuristic.

## GPU Count & Hardware

To evaluate the impact of GPU count, we present the performance of Batch IDA\* with different numbers of GPUs in Table 3, using another server for this experiment. In both domains, performance improves with additional GPUs, with the 4-GPU version matching AIDA\*'s performance on the Rubik's Cube. However, the performance gains diminish with increasing GPU counts, due to fewer threads being available to populate batches. Additionally, we assess Batch IDA\* using various hardware configurations, with results provided in the Supplementary Material.

## PDB Comparison

We conclude by evaluating neural heuristics in Batch IDA\* against AIDA\*. Batch algorithms rely on admissible neural network heuristic  $h_M$ , while non-learning algorithms use a compressed PDB heuristic  $h_{DIV}$  of equal size. Results for STP and Rubik's Cube are presented in Table 4 and Table 5, respectively. The slower performance of learning algorithms compared to the results in Table 1 is due to the need for additional tensor operations per node to ensure heuristic admissibility. Non-learning algorithms expand more nodes in both domains since  $h_{DIV}$  is a weaker heuristic than  $h_M$ . AIDA\* performs significantly better than all other algorithms, while among the learning algorithms, Batch IDA\* remains faster than Batch A\* in terms of constant time per node. We provide a Detailed analysis of this performance gap between AIDA\* and Batch IDA\* in the Supplementary Material.

## Discussion and Conclusions

This paper has shown how to parallelize CB-DFS on the CPU and GPU for efficiently using NN heuristics during search. CB-DFS is explored with Batch IDA\*, but could also be in used in BTS if needed. The batching approach provides significant gains when batch sizes reach a sufficiently large size. Thus, this work provides the foundation for future research on building neural heuristics.



## Acknowledgments

This work was supported by the National Science and Engineering Research Council of Canada Discovery Grant Program and the Canada CIFAR AI Chairs Program. This research was enabled in part by support provided by Prairies DRI and the Digital Research Alliance of Canada (alliance-can.ca). We extend deepest appreciation to our colleague who contributed significant feedback to improving this work.

## References

- Agostinelli, F.; McAleer, S.; Shmakov, A.; and Baldi, P. 2019. Solving the Rubik’s cube with deep reinforcement learning and search. *Nature Machine Intelligence*, 1(8): 356–363.
- Agostinelli, F.; McAleer, S.; Shmakov, A.; Fox, R.; Valtorta, M.; Srivastava, B.; and Baldi, P. 2021. Obtaining approximately admissible heuristic functions through deep reinforcement learning and A\* search. In *Bridging the Gap between AI Planning and Reinforcement Learning workshop at ICAPS*.
- Agostinelli, F.; Shperberg, S. S.; Shmakov, A.; McAleer, S.; Fox, R.; and Baldi, P. 2024. Q\* Search: Heuristic Search with Deep Q-Networks.
- Archetti, A.; Cannici, M.; and Matteucci, M. 2021. Neural weighted a\*: Learning graph costs and heuristics with differentiable anytime a. In *International Conference on Machine Learning, Optimization, and Data Science*, 596–610. Springer.
- Arfaee, S. J.; Zilles, S.; and Holte, R. C. 2011. Learning heuristic functions for large state spaces. *Artificial Intelligence*, 175(16-17): 2075–2098.
- Dally, W. J.; Keckler, S. W.; and Kirk, D. B. 2021. Evolution of the graphics processing unit (GPU). *IEEE Micro*, 41(6): 42–51.
- Ebendt, R.; and Drechsler, R. 2009. Weighted A\* search—unifying view and application. *Artificial Intelligence*, 173(14): 1310–1342.
- Edelkamp, S.; and Sulewski, D. 2009. Parallel state space search on the GPU. In *Symposium on Combinatorial Search*.
- Felner, A.; Korf, R. E.; Meshulam, R.; and Holte, R. C. 2007. Compressed pattern databases. *Journal of Artificial Intelligence Research*, 30: 213–247.
- Felner, A.; Sturtevant, N. R.; and Schaeffer, J. 2009. Abstraction-Based Heuristics with True Distance Computations. In *SARA*.
- Felner, A.; Zahavi, U.; Holte, R.; Schaeffer, J.; Sturtevant, N.; and Zhang, Z. 2011. Inconsistent heuristics in theory and practice. *Artificial Intelligence*, 175(9-10): 1570–1603.
- Hart, P. E.; Nilsson, N. J.; and Raphael, B. 1968. A formal basis for the heuristic determination of minimum cost paths. *IEEE transactions on Systems Science and Cybernetics*, 4(2): 100–107.
- Helmert, M.; Lattimore, T.; Lelis, L. H. S.; Orseau, L.; and Sturtevant, N. R. 2019. Iterative Budgeted Exponential Search. In *International Joint Conference on Artificial Intelligence*, 1249–1257.
- Helmert, M.; Sturtevant, N.; and Felner, A. 2017. On variable dependencies and compressed pattern databases. In *Proceedings of the International Symposium on Combinatorial Search*, volume 8, 129–133.
- Horie, S.; and Fukunaga, A. 2017. Block-parallel IDA\* for GPUs. In *Proceedings of the International Symposium on Combinatorial Search*, volume 8, 134–138.
- Jeon, H. 2023. GPU Architecture. In *Handbook of Computer Architecture*, 1–29. Springer.
- Kaur, J.; and Sturtevant, N. R. 2022. Efficient Budgeted Graph Search. *International Joint Conference on Artificial Intelligence (IJCAI)*.
- Korf, R. E. 1985. Depth-first iterative-deepening: An optimal admissible tree search. *Artificial intelligence*, 27(1): 97–109.
- Li, T.; Chen, R.; Mavrin, B.; Sturtevant, N. R.; Nadav, D.; and Felner, A. 2022. Optimal search with neural networks: Challenges and approaches. In *Proceedings of the International Symposium on Combinatorial Search*, volume 15, 109–117.
- Pándy, M.; Qiu, W.; Corso, G.; Veličković, P.; Ying, Z.; Leskovec, J.; and Liò, P. 2022. Learning graph search heuristics. In *Learning on Graphs Conference*, 10–1. PMLR.
- Pohl, I. 1970. Heuristic search viewed as path finding in a graph. *Artificial intelligence*, 1(3-4): 193–204.
- Reinefeld, A.; and Schnecke, V. 1994. AIDA\*-Asynchronous Parallel IDA\*. In *Canadian Society for Computational Studies of Intelligence*, 295–302.
- Rotem, E.; Yoaz, A.; Rappoport, L.; Robinson, S. J.; Mandelblat, J. Y.; Gihon, A.; Weissmann, E.; Chabukswar, R.; Basin, V.; Fenger, R.; et al. 2022. Intel alder lake CPU architectures. *IEEE Micro*, 42(3): 13–19.
- Samadi, M.; Siabani, M.; Felner, A.; and Holte, R. 2008. Compressing pattern databases with learning. In *ECAI 2008*, 495–499. IOS Press.
- Schrittwieser, J.; Antonoglou, I.; Hubert, T.; Simonyan, K.; Sifre, L.; Schmitt, S.; Guez, A.; Lockhart, E.; Hassabis, D.; Graepel, T.; et al. 2020. Mastering atari, go, chess and shogi by planning with a learned model. *Nature*, 588(7839): 604–609.
- Sturtevant, N.; and Helmert, M. 2020. A Guide to Budgeted Tree Search. In *Symposium on Combinatorial Search (SoCS)*.
- Thayer, J.; Dionne, A.; and Ruml, W. 2011. Learning inadmissible heuristics during search. In *Proceedings of the International Conference on Automated Planning and Scheduling*, volume 21, 250–257.
- Yao, S.; Yu, D.; Zhao, J.; Shafran, I.; Griffiths, T.; Cao, Y.; and Narasimhan, K. 2024. Tree of thoughts: Deliberate problem solving with large language models. *Advances in Neural Information Processing Systems*, 36.
- Yonetani, R.; Tani, T.; Barekatin, M.; Nishimura, M.; and Kanezaki, A. 2021. Path planning using neural a\* search. In *International conference on machine learning*, 12029–12039. PMLR.

Zhou, Y.; and Zeng, J. 2015. Massively parallel A\* search on a GPU. In *AAAI conference on artificial intelligence*.

## Appendix

In this section, we first present the results for the average batch size during runtime. Next, we examine the performance difference between Batch IDA\* and AIDA\*, considering their similar search procedures. Finally, we provide additional results with various hardware configurations to further assess the robustness of Batch IDA\*.

### Batch Size in Practice

As discussed earlier, the batch size during runtime is not always consistent. This occurs because CPU threads may not be able to fully populate the batch when there are only a few pieces of work remaining in the queue. Additionally, in the initial iterations with low cost thresholds, a significant portion of nodes are pruned, resulting in fewer nodes being collected within the specified timeout than the target batch size. Figure 4 shows the average batch size and total number of batches during runtime for both domains. The target batch size is 8000 for the Rubik’s cube and 500 for STP. In both domains, as the search space grows, the number of batches and their sizes increase. In the STP domain, the maximum average batch size reaches only about half of the target batch size due to deeper trees, more IDA\* iterations, and a lower branching factor. This limitation in batch size prevents full utilization of GPU parallelism, contributing to the reduced speedup observed in STP.

### Comparative Analysis of Batch IDA\* and AIDA\*

In this section, we analyze the performance gap between Batch IDA\* and AIDA\*. Let  $h_M$  represent a neural network heuristic and  $h_{PDB}$  a pattern database (PDB) heuristic. We denote the batch size for  $h_M$  by  $b_{NN}$ . If we assume that we have  $n$  CPU threads, AIDA\* also uses batch strategy as all threads perform PDB lookups in parallel. Thus, AIDA\*’s batch size can be considered  $b_{PDB} = n$ . Suppose each  $h_M$  lookup requires  $t_{NN}$  time. Although  $t_{NN}$  slightly varies with batch size, we assume here that it remains constant across batch sizes. Additionally, we define  $t_{copy}$  as the time required to transfer the batch between CPU and GPU.

For AIDA\*, where all threads perform PDB lookups in parallel without race conditions, the lookup overhead for all threads is comparable to that for a single thread:  $t_{PDB}$  for  $n$  lookups is roughly equivalent to  $t_{PDB}$  for one lookup. Now, we make the following assumption regarding batch sizes in Batch IDA\*:

**Assumption 1.** *The batch size for all  $h_M$  lookups is always  $b_{NN}$ .*

We leave out of scope certain conditions in which CPU threads cannot fill the batches, activating the timeout mechanism. Given Assumption 1, for Batch IDA\* and AIDA\* to achieve comparable timing performance, the following condition must hold:

$$\frac{b_{NN} * t_{PDB}}{b_{PDB}} = \frac{b_{NN} * t_{PDB}}{n} = t_{NN} + 2t_{copy} \quad (2)$$

The left-hand side of Equation 2 represents the time AIDA\* needs to process  $b_{NN}$  nodes, while the right-hand side shows the time for Batch IDA\* to process the same batch. A straightforward approach to improving Batch IDA\* performance is to increase  $b_{NN}$ , which initially yields substantial gains. However, beyond a certain point, further increases offer diminishing returns due to the rise in  $t_{copy}$ . Therefore, other solutions to enhance Batch IDA\* efficiency include minimizing  $t_{NN}$  and  $t_{copy}$ . This can be achieved by employing faster GPUs or optimizing  $h_M$  using the following objective:

$$\begin{aligned} \max_{h_M} \quad & \frac{1}{|S|} \sum_{s \in S} h_M(s), \\ \text{subject to} \quad & h_M(s) \leq h^*(s), \quad \forall s \in S, \\ & |h_M| \text{ is minimized} \end{aligned} \quad (3)$$

This optimization balances the heuristic model size while maintaining admissibility and maximizing the average heuristic value.

### Hardware

In this section, we assess the performance of Batch IDA\* across different hardware configurations, categorized as H1, H2, and H3. Table 6 provides an overview of these configurations, with their comparative analysis as follows:

- CPU performance: H3 > H1 > H2
- GPU performance: H3 > H1 > H2

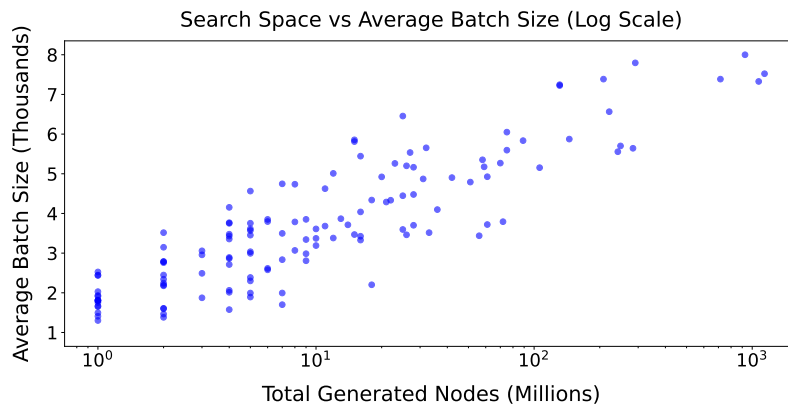
Server	GPU	CPU
H1	GeForce RTX 2080 Ti	AMD Ryzen Threadripper 2950X
H2	GeForce GTX TITAN X	Intel Xeon E5-2620 v3
H3	GeForce RTX A5000	AMD EPYC 7313

Table 6: Details of hardware resources.

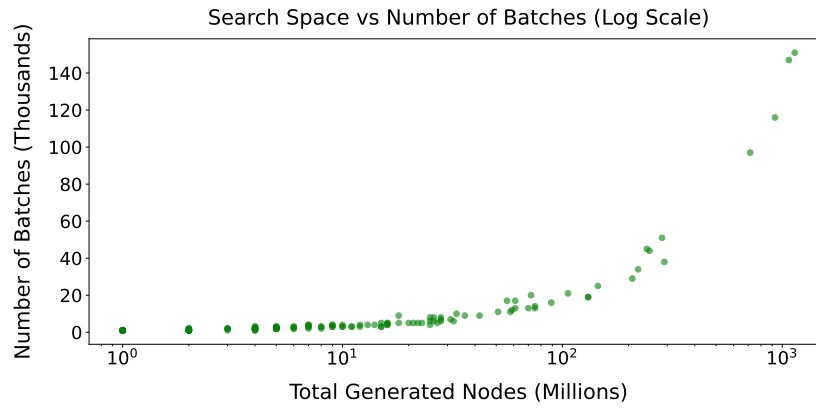
Hardware	Average Time(s) Over 50 Instances			
	SingleGPU Batch IDA*		AIDA*	
	RC	STP	RC	STP
H1	5.87	0.78	2.32	0.026
H2	10.78	1.01	6.81	0.045
H3	4.32	0.60	2.01	0.015

Table 7: Performance across different hardware resources.

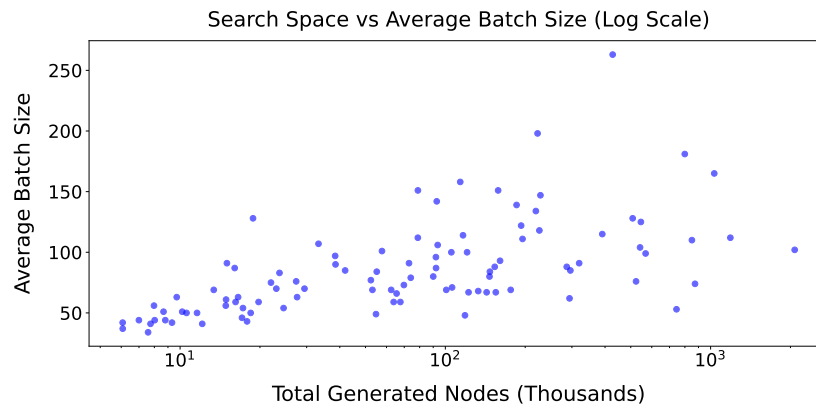
Table 7 presents the performance of SingleGPU Batch IDA\* and AIDA\* across these systems. All systems are configured with 8 threads, due to one server having a maximum of 8 threads. Both methods achieve their best performance on H3 as it has the best CPU and GPU. Although further analysis is required to understand the individual impact of CPU and GPU, these results indicate that AIDA\* is more sensitive to hardware variations, as demonstrated by the more performance gap between H3 and H2 compared to that of Batch IDA\*.



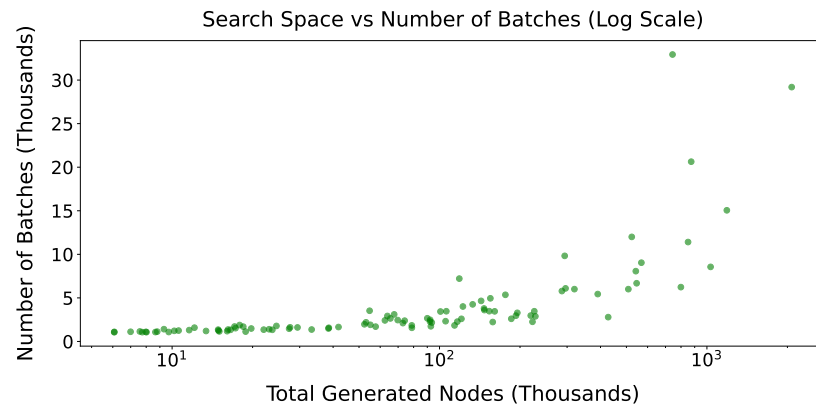
(a) Average batch size in RC



(b) Number of batches in RC



(c) Average batch size in STP



(d) Number of batches in STP

Figure 4: Average batch size and total number of batches during runtime.